



Perovskite Silicon Solar Cell Emulation using Multi-Layer Perceptron Deep Neural Network

Ashraf El-Bardawil^{1,*}, Nehad A. Zidan², Noha H. El-Amary³, W. Abbas¹, Mostafa Fedawy⁴

¹ Basic and Applied Science Department, Faculty of Engineering, Arab Academy for Science, Technology and Maritime Transport, Cairo Governorate 4471344, Egypt

² Mathematics and Physics Department, Faculty of Engineering-Mattaria, Helwan University, Cairo Governorate 4034572, Egypt

³ Electrical and Control Department, Faculty of Engineering, Arab Academy for Science, Technology and Maritime Transport, Cairo Governorate 4471344, Egypt

⁴ Electronics and Communications Department, Faculty of Engineering, Arab Academy for Science, Technology and Maritime Transport, Cairo Governorate 4471344, Egypt

⁵ Center of Excellence in Nanotechnology, Arab Academy for Science, Technology and Maritime Transport, Cairo Governorate 4471344, Egypt

ARTICLE INFO

ABSTRACT

Article history:

Received 20 December 2023

Received in revised form 11 April 2024

Accepted 29 April 2024

Available online 5 July 2024

Keywords:

Multi-layer perceptron (MLP); Perovskite solar cells (PSCs); Photovoltaic cell structure; Power conversion efficiency (PCE)

Perovskite silicon solar cells have an unprecedentedly high-power conversion efficiency compared to other solar cell technologies. This manuscript aims to accomplish two specific goals. The first objective is to investigate the impact of perovskite layer thickness and doping concentration on the solar cell's power conversion efficiency. The second one is to conduct a comparative study to identify the best artificial intelligence technique for simulating the complex nonlinear behaviour of the variation of material parameters versus power conversion efficiency. A solar cell capacitance simulator is used to examine the photovoltaic properties of perovskite silicon solar cells. The simulation is conducted in three stages. Firstly, studying the silicon base structure efficiency to determine the absorber layer c-Si(p) thickness and doping, and the buffer layer c-Si (n) thickness and doping. The second stage is the single-junction of solar cell structure in which c-Si (p++) is used as back surface field. Finally, the perovskite silicon solar cells study the impact of perovskite layer thickness and carrier concentration on power conversion efficiency. The efficiency increases linearly from 26.5% to 28.5% with the perovskite layer thickness. Solar cell behaviour is simulated utilizing multi-layer perceptron. It represents satisfied results.

1. Introduction

Global environmental concerns and rising energy demand, along with continuing advancements in renewable energy technologies, are pushing the use of alternative energy supplies. Nowadays solar energy is the most economical and plentiful long-term natural resource [1-3]. Solar Photovoltaic (PV) technology is one of the best ways to use solar power to create electricity by converting sunlight to direct current in solar cells or PV cells [3,4].

* Corresponding author.

E-mail address: eng_ashraf@aast.edu

<https://doi.org/10.37934/araset.48.1.5160>

Perovskite Solar Cells (PSCs) have gained popularity due to their cheaper cost and easier production techniques. Perovskite materials have been known for a long time, but in 2009, A. Kojima *et al.*, showed the first plan for the solar cell [5,6]. As electron transport material, the nanocrystals of organometallic halide perovskites $\text{CH}_3\text{NH}_3\text{BX}_3$ (B= Sn, Pb; X = Cl, Br, I) that are linked to mesoporous TiO_2 films have been used. These materials absorb light in a good manner and have efficiencies up to 3.8% and 3.13% respectively [6,7]. A summarizing brief is given here to show what has happened to the percentage of each of the PCE for 2 terminal perovskite-silicon based solar cells according to the simulation results that are already validated in [8-15]. Sahli *et al.*, had reached 25.2 % for the power conversion efficiency by 6/2018 [8]. While Mazzarella *et al.*, had the same level of percentage for PCE which is exactly 25.2 % by 2/2019 [9], although Köhnen *et al.*, had a slight diminution in the percentage that reach for PCE to 25.1% by 5/2019 [10]. In August 2020 Nayan Das, Rishav Paul, have improved the PCE to 27% [11]. Amri *et al.*, reached PCE to 24.4 in 6/2021 [12-15].

Machine learning models can get around the problems with econometric models and consider non-linear features, they have been used many times for forecasting in the past few years [16-19]. Multi-Layer Perceptron Deep Neural Network (MLP-DNN) is a typical feedforward neural network with one or more layers between the input and output layers. MLP is beneficial due to its capacity to resolve both classification and regression [20-24].

This manuscript illustrates the effect of studying the perovskite/silicon solar cell's structure factors that limit its performance. There are different evaluating parameters for the perovskite/silicon solar cells structure like the influence of the absorber layer thickness, the absorber layer doping, the buffer layer thickness and the buffer layer doping. Furthermore, obtaining the optimum highest possible short-circuit current density (J_{sc}), open-circuit voltage (V_{oc}), and fill factor (FF) can be calculated from the evaluating parameters mentioned before. MLP-DNN is implemented to model the non-linear PV internal parameters. Comparing the results of this paper to the other manuscripts findings, the cell PCE is improved to 28.2% instead of 23.92% without perovskite layer, in addition to the usage of the MLP-DNN. PCE is achieved using the variation of parameters.

The presented paper is organized as follows: Section I includes the manuscript Introduction. Section II presents the mathematical model. Section III discusses the simulation and results, and section IV illustrates Multi-Layer Perceptron Deep Neural Network. Finally, section V concludes the paper.

2. Methodology

The Solar Cell Capacitance Simulator SCAPS-1D is utilized to analyse different kinds of solar cells and can simulate PSC [25]. In comparison with other tools, SCAPS has a relatively easy-to-use operating window and different kinds of models for grading, defects, and recombination [26].

SCAPS software is utilized to solve the basic equations of a semiconductor, such as the continuity equation for electrons and holes, the transport equation, and Poisson's equation [27]. The continuity equations for electron and hole concentration change are expressed by Eq. (2) and Eq. (3) [28]. SCAPS can solve structures with up to eight layers and two contacts. Each layer can have its own set of parameters for all kinds of materials. It can analysis and simulate the J-V characteristics curve, spectral response of the device, PCE, Fill Factor (FF), short-circuit current (J_{sc}), and open circuit voltage (V_{oc}) [29].

$$\frac{\partial^2 \phi}{\partial x^2} = \frac{q}{\epsilon} [n(x) - p(x) - N_D^+(x) + N_A^-(x) - p_t(x) + n_t(x)] \quad (1)$$

$$\frac{\partial n}{\partial t} = \frac{1}{q} \frac{\partial J_n}{\partial x} + (G_n - R_n) \quad (2)$$

$$\frac{\partial p}{\partial t} = \frac{1}{q} \frac{\partial J_p}{\partial x} + (G_p - R_p) \quad (3)$$

Where:

φ :	the potential	$n_t(x)$:	the trapped electron density
q :	the elementary charge	G_n :	the optical generation rate of electrons
ε :	the permittivity	G_p :	the optical generation rate of holes
n :	the free electron density	R_n :	the recombination rate of electrons
p :	the free hole density	R_p :	the recombination rate of holes
N_D^+ :	the donor density	J_n :	the electron current density
$p_t(x)$:	the trapped hole density	J_p :	the hole current density
$N_A^-(x)$:	the acceptor density		

3. Simulation and Results

The simulation is divided into three sections. Firstly, the silicon base structure is studied which consists of the absorber layer (c-Si (p)) and the buffer layer (c-Si (n)) [30]. Secondly the silicon base structure with Back Surface Field (BSF). Finally, the factors that limit the performance of perovskite/silicon solar cells are studied.

3.1 Silicon Base Solar Cell Structure

While the main parameters that are used to characterize the performance of solar cells are V_{OC} , J_{SC} , F.F and PCE. The cell structure is consisting of c-Si (p) as absorber layer, c-Si (n) as the buffer layer, the surface is covered with a layer (anti reflected coating) to avoid light loss, and there is a contact layer on the top and bottom of the cell to complete the circuit as indicates in Figure 1.

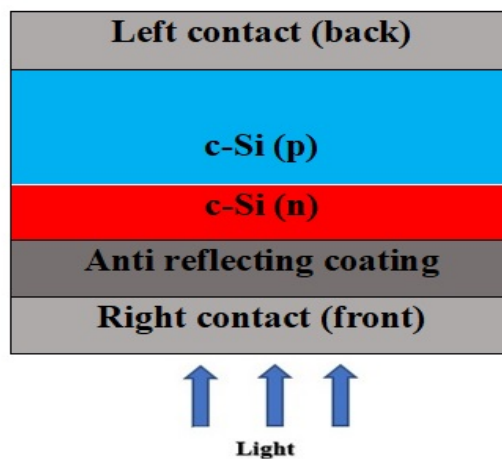


Fig. 1. Basic structure of the solar cell

The variation of PCE with the buffer layer thickness (t_n), the absorber layer thickness (t_p), the absorber layer doping (N_A) and buffer layer doping (N_D) is illustrated in Figure 2 (a, b, c, and d) respectively. It is obvious that the optimum thickness for the absorber layer and the buffer layer is $250 \mu m$ and $100 nm$ respectively. To be considered as the reference parameters for the simulation

studied, the PCE is approximately equal to 22.5% as $t_p = 250 \mu\text{m}$, $t_n = 100 \text{ nm}$, $N_A = 10^{19} \text{ cm}^{-3}$, and $N_D = 10^{20} \text{ cm}^{-3}$.

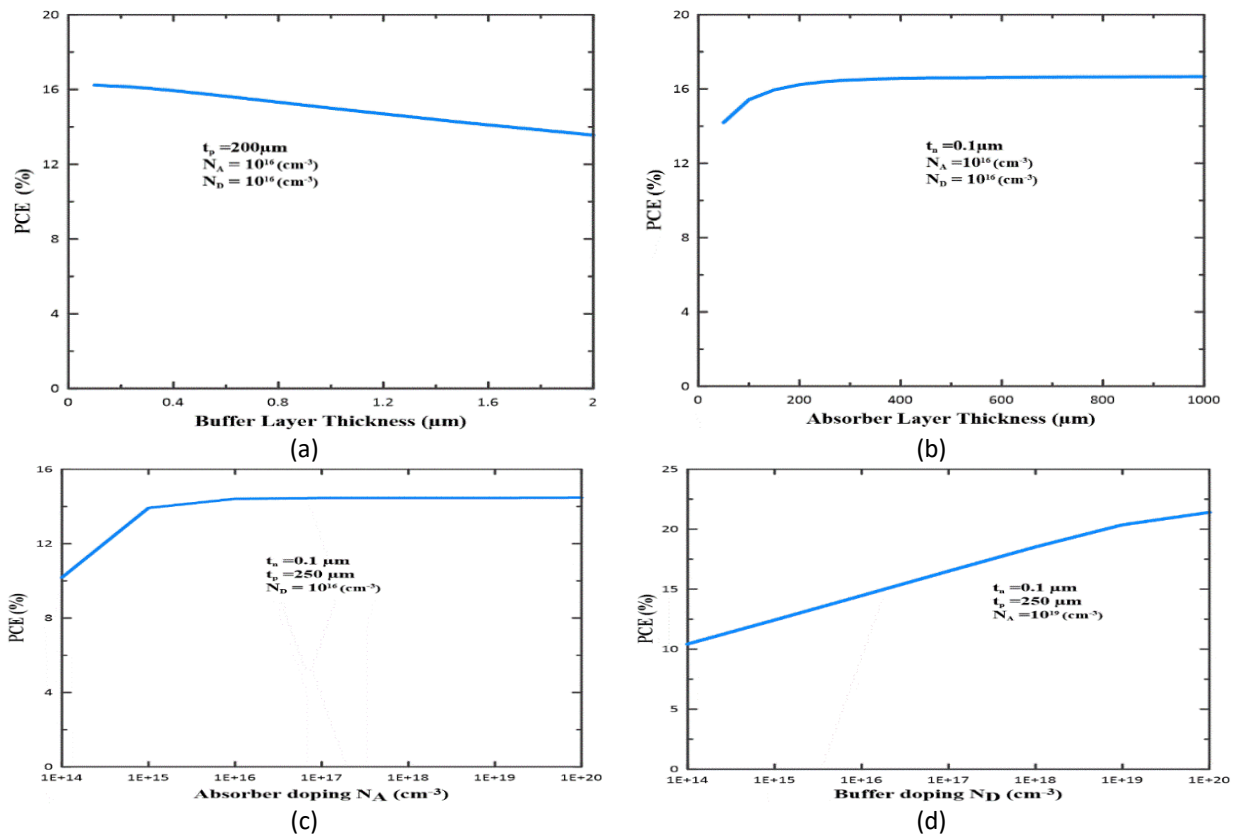


Fig. 2. (a) Buffer layer thickness vs PCE, (b) Absorber layer thickness vs PCE, (c) Absorber layer doping vs PCE and (d) Buffer layer doping vs PCE

3.2 Single Junction Solar Cell Structure

The single-junction of solar cell structure in which c-Si (p++) is used as Back Surface Field (BSF), c-Si (p) as absorber layer and c-Si (n) as the buffer layer is clarified in Figure 3. The thickness of c-Si (p++) layer is varied from 10 nm to 500 nm.

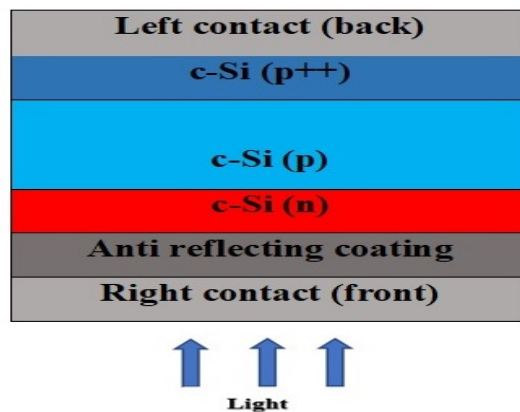


Fig. 3. Single junction solar cell structure

The relation between BSF layer thickness (in nm) versus V_{oc} (in v), J_{sc} (in mA/cm^2), PCE (in %) and F.F (in %) is illustrated in Figure 4 (a and b). It is obvious that the PCE and J_{sc} increase linearly as BSF thickness increases, while fill factor remains constant. The PCE is approximately equal to 23.92%, There are two major benefits that may be obtained. by utilizing this back surface filed c-Si (p++):

- i. A small improvement in the PCE can be observed.
- ii. The absorber layer thickness has been decreased from 250 to 100 μm that will reduce the cost of industrialization.

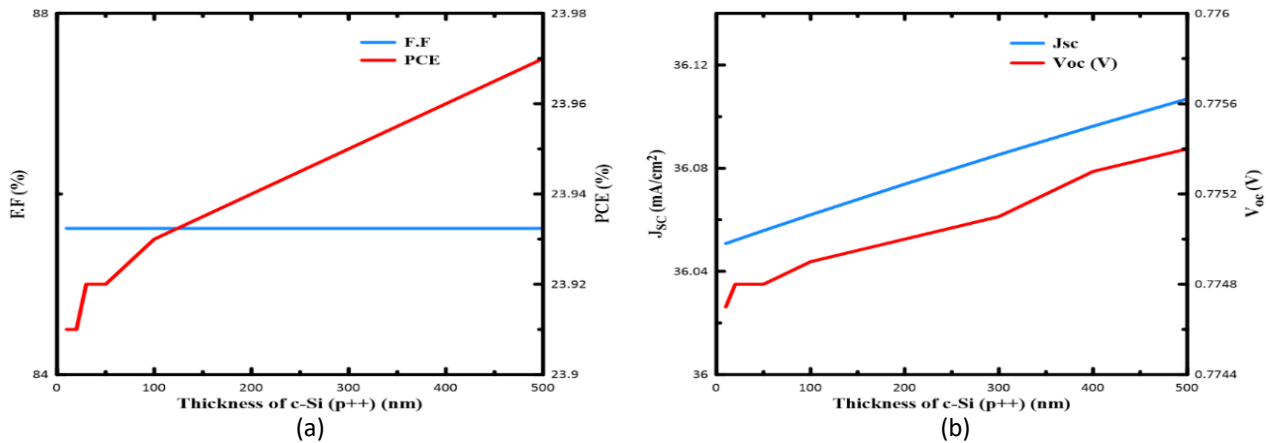


Fig. 4. (a) BSF layer thickness vs power conversion efficiency and fill factor, (b) BSF layer thickness vs open circuit voltage and short circuit current density

3.3 Perovskite/Silicon Solar Cell

Organometallic halide perovskite solar cells are recently used extensively due to their high carrier mobility, intense light absorption coefficient and their long carrier diffusion length. Figure 5 shows that an additional layer is added to the single junction structure of solar cell. The structure composition of Fluorine-doped Tin Oxide (FTO), methylammonium tin halides ($CH_3NH_3SnI_3$) Perovskite, c-Si (n), c-Si (p) and c-Si (p++). Anti reflected coating FTO is chosen due to high transparency, low manufacturing cost, large energy gap and thermal stability. The $CH_3NH_3SnI_3$ is chosen for the overall structure due to its simple manufacturing technique and higher PCE than conventional organic solar cells. The effect of perovskite layer thickness and doping on PCE is discussed in the next section.

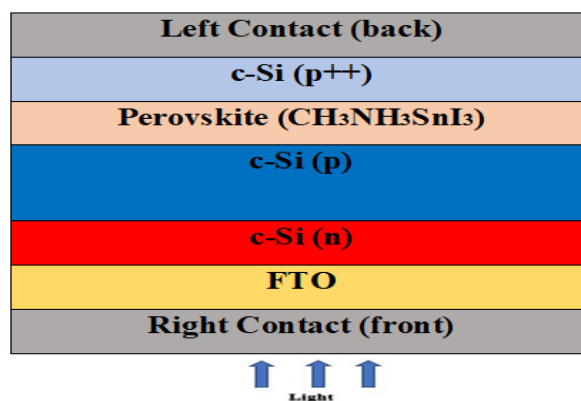


Fig. 5. Structure of perovskite/silicon solar cell

3.3.1 Perovskite layer thickness (t_{PRVS})

There are different parameters that can be utilized to maximize the PCE, the perovskite layer thickness t_{PRVS} is one of these parameters which is used in this study. t_{PRVS} varied from 10 to 1000 nm. Figure 6 (a and b) shows the relation between the t_{PRVS} (in nm) versus V_{oc} (in v), J_{sc} (in mA/cm^2), PCE (in %) and F.F (in %). It is noticed that the PCE increases linearly as t_{PRVS} thickness increases until PCE = 28.45%.

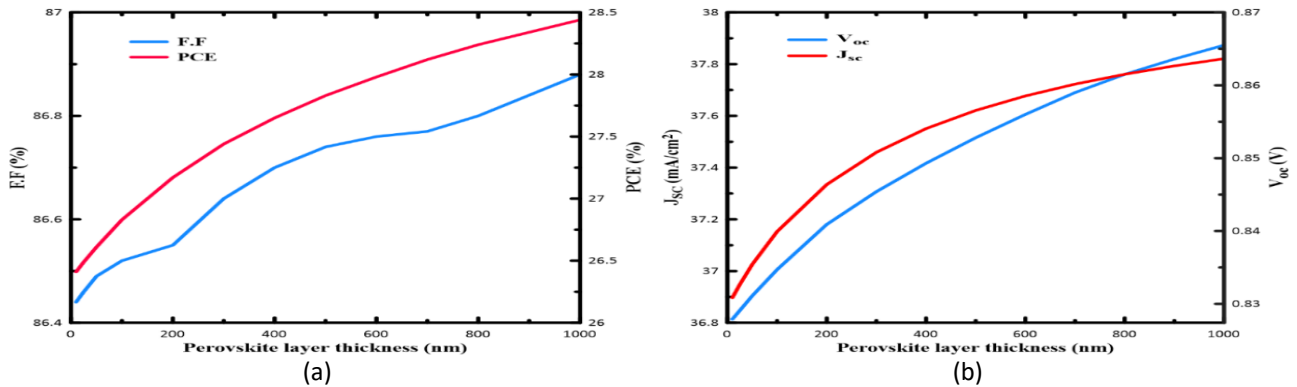


Fig. 6. (a) Perovskite layer thickness vs power conversion efficiency and fill factor, (b) Perovskite layer thickness vs open circuit voltage and short circuit current density

3.3.2 Perovskite layer doping (N_{PRVS})

The perovskite layer doping N_{PRVS} is varied from 10^{13} to $10^{20} cm^{-3}$. The relation between N_{PRVS} (in cm^{-3}) versus V_{oc} (in v), J_{sc} (in mA/cm^2), PCE (in %) and F.F (in %) is illustrated in Figure 7. It is obvious that the PCE and F.F increase from 27% to 30.6% and 85.6% to 87.4% respectively, as N_{PRVS} increases.

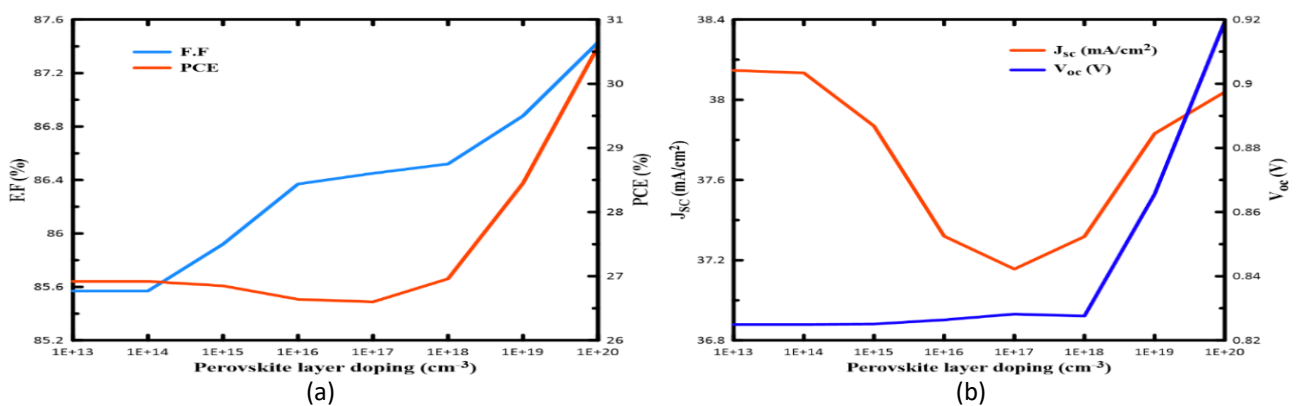


Fig. 7. (a) Perovskite doping vs power conversion efficiency and fill factor, (b) Perovskite doping vs open circuit voltage and short circuit current density

Table 1 presents the main parameters of overall structures of the solar cell such as thickness, bandgap, electron affinity, dielectric permittivity, hole thermal velocity, etc.

Table 1
 Material parameters of the developed solar cell

Parameters	FTO	c-Si (n)	c-Si (p)	CH ₃ NH ₃ SnI ₃	c-Si (p++)
Thickness	100 nm	150 nm	85 μm	1 μm	50 nm
bandgap (eV)	3.5	1.124	1.124	1.3	1.124
electron affinity (eV)	4	3.900	4.05	4.17	3.9
dielectric permittivity (relative)	9	11.900	11.900	8.2	11.900
CB effective density (cm^{-3})	$2.2 \cdot 10^{19}$	$2.8 \cdot 10^{19}$	$2.8 \cdot 10^{19}$	10^{18}	$2.8 \cdot 10^{19}$
VB effective density (cm^{-3})	$1.8 \cdot 10^{18}$	$1.04 \cdot 10^{19}$	$1.04 \cdot 10^{19}$	10^{19}	$1.04 \cdot 10^{19}$
electron thermal velocity (cm/s)	$1 \cdot 10^7$	$2.03 \cdot 10^7$	$2.03 \cdot 10^7$	10^7	$2.03 \cdot 10^7$
hole thermal velocity (cm/s)	$1 \cdot 10^7$	$1.67 \cdot 10^7$	$1.67 \cdot 10^7$	10^7	$1.67 \cdot 10^7$
electron mobility (cm^2/Vs)	20	1250	1010	1.6	1212
hole mobility (cm^2/Vs)	10	443	443	1.6	421
Acceptor concentration (cm^{-3})	0	0	10^{19}	10^{19}	10^{21}
Donor concentration (cm^{-3})	10^{19}	10^{20}	0	0	0

Figure 8 indicates the J-V curve of the solar cell. It is cleared that $V_{oc} = 0.8656$ v and $J_{sc} = 37.83$ mA/cm².

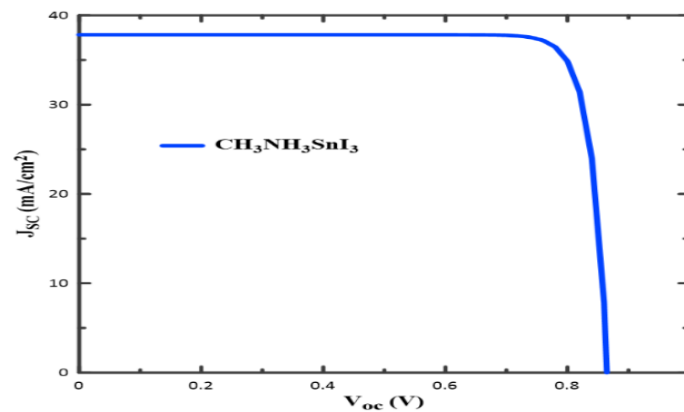


Fig. 8. Open circuit voltage vs short circuit current density of the solar cell

4. Multi-Layer Perceptron Deep Neural Network

In this paper, MLP-DNN technique is used to predict the value of PCE for the designed solar cells, based on the non-linear PV internal parameters behaviour. The system consists of six input features (t_n , t_p , t_{PRVS} , t_{p++} , N_A and N_d) and one output (PCE).

The dataset used to train and test the proposed system is created using SCAPS. It consists of 613 samples. The training dataset consists of 80% of the samples, while 20% are used to test the trained model.

The MLP is a class of feedforward neural networks which consists of at least three different layers. The first layer is the input layer where the samples are fed to the MLP model. The size of this layer depends mainly on the number of features (PV internal parameters). The size of the output layer depends on the number of predicted outputs, which is set to one (PCE) in the designed model. MLPs usually have a single hidden layer, however when this number of hidden layer increases, the architecture transforms to what is known as DNN. The MLP neural network architecture consists of 7 layers (one input, five hidden layers, and one output), and all the layers are dense (fully connected). When compared to Artificial Neural Networks (ANN) for regression, linear regression is limited in its ability to learn complicated non-linear relationships between the input features and outputs, which

is why ANNs are preferred. Therefore, new methods to discover the intricate non-linear connection between the PV internal parameters and the PCE are investigated. ANNs, such as the proposed MLP architecture, are one of these methods. As an activation function is embedded into each layer of the artificial neural network, it is possible for the network to understand the intricate connection between the inputs and the outputs. The numbers and sizes of hidden layers, and the activation function of the MLP neural networks are considered as hyper-parameters. They can affect how fast the MLP architecture can be trained and can also affect the accuracy of the prediction results. In order to select the optimum hyper-parameters for the proposed architecture, a simple grid-search technique is used, in which the system is trained for 500 epochs. The hyper-parameters that yield the lowest Mean Absolute Error (MAE) are selected to train the MLP model. The general architecture of MLP is illustrated in Figure 9.

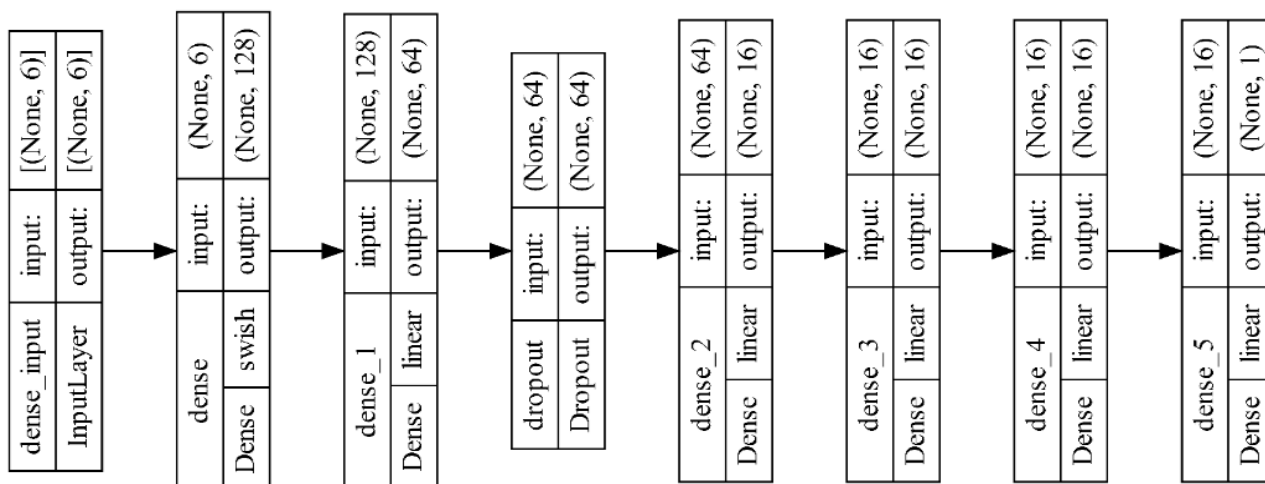


Fig. 9. Multilayer perceptron regression architecture

The achieved Root Mean Square Error (RMSE) for the predicted PCE is equal to 0.24. Figure 10 illustrates the values of predicted and original PCE. The predicted results can be considered as a satisfactory output with an acceptable RMSE.

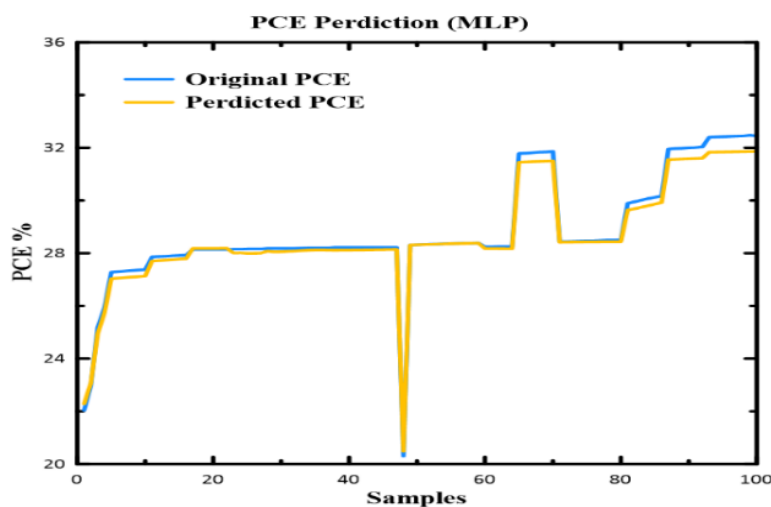


Fig. 10. The predicted and original power conversion efficiency variation with the test samples using MLP-DNN

5. Conclusions

Referring to the sustainable development goals and the recommendation of COP27, this paper targets to reach the best power conversion efficiency of the solar cell based on cutting-edge technology. Organometallic halide perovskite solar cell is studied in this work, through three stages and varying its internal parameters. The first stage aims to find the higher PCE of the silicon base cell structure. In the second stage, the back surface field is added to get better PCE. Finally, adding the perovskite layer to the solar cell structure to give a fill factor of 86.87%, and PCE of 28.2% compared to 22.5% for the silicon base structure PCE. The results of the three stages and the optimal parameters of the PSC structure, as top and bottom cell layer thickness, and carrier concentration are trained, validated, and tested to MLP-DNN AI technique. The actual Root Mean Square Error (RMSE) for the predicted PCE is 0.24.

Acknowledgement

This research was not funded by any grant.

References

- [1] Obaideen, Khaled, Maryam Nooman AlMallahi, Abdul Hai Alami, Mohamad Ramadan, Mohammad Ali Abdelkareem, Nabila Shehata, and A. G. Olabi. "On the contribution of solar energy to sustainable developments goals: Case study on Mohammed bin Rashid Al Maktoum Solar Park." *International Journal of Thermofluids* 12 (2021): 100123. <https://doi.org/10.1016/j.ijft.2021.100123>
- [2] Akter, Farzana, Kazi Ahasan Ekram, Md Araful Hoque, and Mohammad Joynal Abedin. "An Assessment of Solar Micro-Grid System in the Islands of Bangladesh for Sustainable Energy Access." *Malaysian Journal on Composites Science and Manufacturing* 12, no. 1 (2023): 31-42. <https://doi.org/10.37934/mjcsms.12.1.3142>
- [3] Amran, Mohd Effendi, and Mohd Nabil Muhtazaruddin. "Renewable Energy Optimization Review: Variables towards Competitive Advantage in Green Building Development." *Progress in Energy and Environment* (2019): 1-15.
- [4] Ahmad, Nur Irwany, Vernon Yeoh Sheng Liang, Diyaa Hidayah Abd Rahman, Aimi Athirah Hazwani Zaidi, Saidatul Shema Saad, Nazrul Azril Nazlan, Habibah Mokhtaruddin, and Baseemah Mat Jalaluddin. "Development of Solar Tracking Robot for Improving Solar Photovoltaic (PV) Module Efficiency." *Journal of Advanced Research in Applied Mechanics* 61, no. 1 (2019): 13-24.
- [5] Hindi, Noor Abbas, Saadoon Fahad Dakhil, and Karrar Abdullah Abbas. "Experimental Study to Improve Solar Photovoltaic Performance by Utilizing PCM and Finned Wall." *Journal of Advanced Research in Fluid Mechanics and Thermal Sciences* 102, no. 1 (2023): 153-170. <https://doi.org/10.37934/arfmts.102.1.153170>
- [6] Hima, Abdelkader, Nacereddine Lakhdar, Boubaker Benhaoua, Achour Saadoun, Imad Kemerchou, and Fatiha Rogti. "An optimized perovskite solar cell designs for high conversion efficiency." *Superlattices and Microstructures* 129 (2019): 240-246. <https://doi.org/10.1016/j.spmi.2019.04.007>
- [7] Nowsherwan, Ghazi Aman, K. Jahangir, Y. Usman, W. Saleem, and Md Khalid. "Numerical Modeling and Optimization of Perovskite Silicon Tandem Solar Cell Using SCAPS-1D." *Sch Bull* 7, no. 7 (2021): 171-184. <https://doi.org/10.1155/2021/6668687>
- [8] Sahli, Florent, Jérémie Werner, Brett A. Kamino, Matthias Bräuninger, Raphaël Monnard, Bertrand Paviet-Salomon, Loris Barraud *et al.*, "Fully textured monolithic perovskite/silicon tandem solar cells with 25.2% power conversion efficiency." *Nature materials* 17, no. 9 (2018): 820-826. <https://doi.org/10.1038/s41563-018-0115-4>
- [9] Mazzarella, Luana, Yen-Hung Lin, Simon Kirner, Anna B. Morales-Vilches, Lars Korte, Steve Albrecht, Ed Crossland *et al.*, "Infrared light management using a nanocrystalline silicon oxide interlayer in monolithic perovskite/silicon heterojunction tandem solar cells with efficiency above 25%." *Advanced Energy Materials* 9, no. 14 (2019): 1803241. <https://doi.org/10.1002/aenm.201803241>
- [10] Köhnen, Eike, Marko Jošt, Anna Belen Morales-Vilches, Philipp Tockhorn, Amran Al-Ashouri, Bart Macco, Lukas Kegelman *et al.*, "Highly efficient monolithic perovskite silicon tandem solar cells: analyzing the influence of current mismatch on device performance." *Sustainable Energy & Fuels* 3, no. 8 (2019): 1995-2005. <https://doi.org/10.1039/C9SE00120D>
- [11] Das, Nayan, and Rishav Paul. "Design And Optimisation Of Lead Free Perovskite/Silicon Tandem Solar Cell Using Scaps-1D Software."

- [12] Amri, Khaoula, Rabeb Belghouthi, Michel Aillerie, and Rached Gharbi. "Device optimization of a lead-free perovskite/silicon tandem solar cell with 24.4% power conversion efficiency." *Energies* 14, no. 12 (2021): 3383. <https://doi.org/10.3390/en14123383>
- [13] Mostafa, Ola, Nehad A. Zidan, Wael Abbas, Hanady Hussein Issa, Nihal Gamal, and Mostafa Fedawy. "Design and Performance Optimization of Lead-Free Perovskite Solar Cells with Enhanced Efficiency." *Mathematical Modelling of Engineering Problems* 10, no. 4 (2023). <https://doi.org/10.18280/mmep.100424>
- [14] Dawoud, Mina, M. Aboul-Dahab, S. H. Zainud-Deen, and H. A. Malhat. "Tapered Metal Nanoantenna Structures for Absorption Enhancement in GaAs Thin-Film Solar Cells." *Journal of Advanced Research in Applied Mechanics* 44, no. 1 (2018): 1-7.
- [15] El-Mahalawy, Ahmed M., W. Abbas, Ola Mostafa, Nehad A. Zidan, Hanady Hussein Issa, M. Fedawy, and Ahmed R. Wassel. "Integrative role of PEDOT: PSS in adjusting the photoresponse efficiency of novel reduced graphene quantum dots/silicon heterojunction for optoelectronics and solar energy conversion applications." *Surfaces and Interfaces* 46 (2024): 103946. <https://doi.org/10.1016/j.surfin.2024.103946>
- [16] Singh, Vijay P., Shalini Yadav, Krishna Kumar Yadav, Gerald Augusto Corzo Perez, Francisco Muñoz-Arriola, and Ram Narayan Yadava, eds. *Application of Remote Sensing and GIS in Natural Resources and Built Infrastructure Management*. Springer, 2022. <https://doi.org/10.1007/978-3-031-14096-9>
- [17] Alzubaidi, Laith, Jinglan Zhang, Amjad J. Humaidi, Ayad Al-Dujaili, Ye Duan, Omran Al-Shamma, José Santamaría, Mohammed A. Fadhel, Muthana Al-Amidie, and Laith Farhan. "Review of deep learning: concepts, CNN architectures, challenges, applications, future directions." *Journal of big Data* 8 (2021): 1-74. <https://doi.org/10.1186/s40537-021-00444-8>
- [18] Quan, Quan, Zou Hao, Huang Xifeng, and Lei Jingchun. "Research on water temperature prediction based on improved support vector regression." *Neural Computing and Applications* (2022): 1-10.
- [19] Eissa, Nouredin S., Uswah Khairuddin, and Rubiyah Yusof. "A hybrid metaheuristic-deep learning technique for the pan-classification of cancer based on DNA methylation." *BMC bioinformatics* 23, no. 1 (2022): 273. <https://doi.org/10.1186/s12859-022-04815-7>
- [20] Costandy, Rana N., Safa M. Gasser, Mohamed S. El-Mahallawy, Mohamed W. Fakhr, and Samir Y. Marzouk. "P-wave detection using a fully convolutional neural network in electrocardiogram images." *Applied Sciences* 10, no. 3 (2020): 976. <https://doi.org/10.3390/app10030976>
- [21] Bahtiyar, Hüseyin, Derya Soydaner, and Esra Yüksel. "Application of multilayer perceptron with data augmentation in nuclear physics." *Applied Soft Computing* 128 (2022): 109470. <https://doi.org/10.1016/j.asoc.2022.109470>
- [22] Esfe, Mohammad Hemmat, Fatemeh Amoozadkhalili, and Davood Toghraie. "Determining the optimal structure for accurate estimation of the dynamic viscosity of oil-based hybrid nanofluid containing MgO and MWCNTs nanoparticles using multilayer perceptron neural networks with Levenberg-Marquardt Algorithm." *Powder Technology* 415 (2023): 118085. <https://doi.org/10.1016/j.powtec.2022.118085>
- [23] Hemmat, Mohammad, Davood Toghraie, and Fatemeh Amoozad. "Prediction of viscosity of MWCNT-Al₂O₃ (20:80)/SAE40 nano-lubricant using multi-layer artificial neural network (MLP-ANN) modeling." *Engineering Applications of Artificial Intelligence* 121 (2023): 105948. <https://doi.org/10.1016/j.engappai.2023.105948>
- [24] Jahan, Sultana, M. Ferdows, M. D. Shamshuddin, and Khairy Zaimi. "Effects of solar radiation and viscous dissipation on mixed convective non-isothermal hybrid nanofluid over moving thin needle." *Journal of Advanced Research in Micro and Nano Engineering* 3, no. 1 (2021): 1-11.
- [25] Burgelman, Marc, Peter Nollet, and Stefaan Degraeve. "Modelling polycrystalline semiconductor solar cells." *Thin solid films* 361 (2000): 527-532. [https://doi.org/10.1016/S0040-6090\(99\)00825-1](https://doi.org/10.1016/S0040-6090(99)00825-1)
- [26] Decock, Koen, Paweł Zabierowski, and Marc Burgelman. "Modeling metastabilities in chalcopyrite-based thin film solar cells." *Journal of Applied Physics* 111, no. 4 (2012). <https://doi.org/10.1063/1.3686651>
- [27] Shawky, Tarek, Moustafa H. Aly, and Mostafa Fedawy. "Performance analysis and simulation of c-Si/SiGe based solar cell." *IEEE Access* 9 (2021): 75283-75292. <https://doi.org/10.1109/ACCESS.2021.3080391>
- [28] Husainat, Ali, Warsame Ali, Penrose Cofie, John Attia, and John Fuller. "Simulation and analysis of methylammonium lead iodide (CH₃NH₃PbI₃) perovskite solar cell with Au contact using SCAPS 1D simulator." *American Journal of Optics and Photonics* 7, no. 2 (2019): 33. <https://doi.org/10.11648/j.ajop.20190702.12>
- [29] Morales-Acevedo, Arturo, Norberto Hernández-Como, and Gaspar Casados-Cruz. "Modeling solar cells: a method for improving their efficiency." *Materials Science and Engineering: B* 177, no. 16 (2012): 1430-1435. <https://doi.org/10.1016/j.mseb.2012.01.010>
- [30] Al Bardawil, Ashraf Saeed, Nehad A. Zidan, Noha H. El-Amary, W. Abbas, and Mostafa Fedawy. "Intelligent Maximization of Eco-friendly Output Energy Based on Internal Photovoltaic Structure." *International Journal of Renewable Energy Research (IJRER)* 13, no. 4 (2023): 1497-1507.